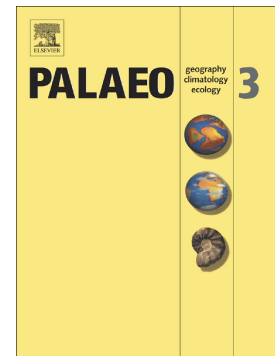


## Accepted Manuscript

A record of Late Ordovician to Silurian oceanographic events on the margin of Baltica based on new carbon isotope data, elemental geochemistry, and biostratigraphy from two boreholes in central Poland

Nicholas B. Sullivan, David K. Loydell, Paul Montgomery, Stewart G. Molyneux, Jan Zalasiewicz, Kenneth T. Ratcliffe, Elaine Campbell, James D. Griffiths, Gavin Lewis



PII: S0031-0182(17)30597-7  
DOI: doi:[10.1016/j.palaeo.2017.10.016](https://doi.org/10.1016/j.palaeo.2017.10.016)  
Reference: PALAEO 8483

To appear in: *Palaeogeography, Palaeoclimatology, Palaeoecology*

Received date: 31 May 2017  
Revised date: 13 October 2017  
Accepted date: 14 October 2017

Please cite this article as: Nicholas B. Sullivan, David K. Loydell, Paul Montgomery, Stewart G. Molyneux, Jan Zalasiewicz, Kenneth T. Ratcliffe, Elaine Campbell, James D. Griffiths, Gavin Lewis , A record of Late Ordovician to Silurian oceanographic events on the margin of Baltica based on new carbon isotope data, elemental geochemistry, and biostratigraphy from two boreholes in central Poland. The address for the corresponding author was captured as affiliation for all authors. Please check if appropriate. *Palaeo*(2017), doi:[10.1016/j.palaeo.2017.10.016](https://doi.org/10.1016/j.palaeo.2017.10.016)

This is a PDF file of an unedited manuscript that has been accepted for publication. As a service to our customers we are providing this early version of the manuscript. The manuscript will undergo copyediting, typesetting, and review of the resulting proof before it is published in its final form. Please note that during the production process errors may be discovered which could affect the content, and all legal disclaimers that apply to the journal pertain.

**A record of Late Ordovician to Silurian oceanographic events on the margin of Baltica based on new carbon isotope data, elemental geochemistry, and biostratigraphy from two boreholes in central Poland**

Nicholas B. Sullivan<sup>a</sup>, David K. Loydell<sup>b</sup>, Paul Montgomery<sup>c</sup>, Stewart G. Molyneux<sup>d</sup>, Jan Zalasiewicz<sup>e</sup>, Kenneth T. Ratcliffe<sup>f</sup>, Elaine Campbell<sup>c</sup>, James D. Griffiths<sup>g</sup>, Gavin Lewis<sup>h</sup>

<sup>a</sup> *Chemostrat Inc., 3760 Westchase Drive, Houston, TX 77057, United States*

<sup>b</sup> *School of Earth and Environmental Sciences, University of Portsmouth, Burnaby Road, Portsmouth PO1 3QL, UK*

<sup>c</sup> *Chevron Energy Technology Company, 1500 Louisiana St., Houston, TX 77002, United States*

<sup>d</sup> *British Geological Survey, Nicker Hill, Keyworth, Nottingham NG12 5GG, UK*

<sup>e</sup> *School of Geography, Geology, and the Environment, University of Leicester, University Road, Leicester LE1 7RH, UK*

<sup>f</sup> *Chemostrat Ltd, Unit 1, Ravenscroft Court, Buttington Cross Enterprise Park, Welshpool SY21 8SL, UK*

<sup>g</sup> *Enzygo Ltd, Samuel House, 5 Fox Valley Way, Stocksbridge, Sheffield S36 2AA, UK*

<sup>h</sup> *Chevron Global Exploration New Ventures, 1500 Louisiana St., Houston, TX 77002, United States*

Corresponding Author: Nicholas B. Sullivan (nbsullivan@wisc.edu)

**Key words:** graptolites; chitinozoans; acritarchs; chronostratigraphy; Paleozoic bioevents; chemostratigraphy

## Abstract

New stable isotope data from organic carbon ( $\delta^{13}\text{C}_{\text{org}}$ ) and inorganic elemental geochemistry data have been generated from Upper Ordovician to Silurian strata in two boreholes in the Lublin Basin of Poland: Grabowiec-6 and Zwierzyniec-1. They have been integrated here with biostratigraphical data from graptolites, acritarchs, and chitinozoans. Faunal assemblages from Grabowiec-6 indicate that it spans from the Katian (*clingani* graptolite Biozone) to the Gorstian (*scanicus* graptolite Biozone);  $\delta^{13}\text{C}_{\text{org}}$  values from this section record the Sheinwoodian Ireviken Excursion, the Homeric Mulde Excursion, and a minor positive shift associated with the lower Ludfordian *leintwardinensis* Biozone. The second section, Zwierzyniec-1, spans the Sandbian through Gorstian (*nilssoni* Biozone);  $\delta^{13}\text{C}_{\text{org}}$  values record the Hirnantian carbon isotope excursion (HICE) and the Ireviken Excursion as well.

Elemental geochemistry data is used to recognize subtle changes in provenance and lithology. Significant increases in the abundance of V and Mo are recognized in strata deposited above the Ireviken Excursion. The enrichment of these redox sensitive elements suggests that persistent regional anoxia and euxinia may be associated with the aftermath of these oceanographic disturbances. Some of these same trace elements, along with  $\text{Fe}_2\text{O}_3$ , and Pb are also abundant in strata coeval with, or just below the Ireviken and HICE excursions. This may

have a causal link with malformed palynomorphs observed at these intervals by some workers, which are thought to reflect toxic levels of dissolved heavy metals in the world's oceans.

ACCEPTED MANUSCRIPT

## 1. Introduction

The Late Ordovician and Silurian periods are punctuated by numerous, widely characterized disturbances of the global climate and oceanographic system. Many of these events were initially defined by extinction events affecting conodonts (Aldridge et al., 1993; Jeppsson, 1993, 1997a, 1998; Männik, 2005, 2007) and graptolites (Štorch, 1995; Melchin et al., 1998; Loydell, 2007). Many are also associated with significant, short-lived positive shifts in stable carbon isotope values (Kaljo et al., 1997, 1998; Munnecke et al., 2003; Kaljo and Martma, 2006).

The cause of these positive “excursions” in the Silurian is a matter of some debate (Saltzman, 2003; Cramer and Saltzman, 2007a; Loydell, 2007, 2008; Cramer and Munnecke, 2008; McLaughlin et al., 2012a; Vandenbroucke et al., 2015), nevertheless, it is generally thought that these phenomena are linked to widespread burial of isotopically light organic carbon ( $^{12}\text{C}$ ) in the deep sea, leaving the atmosphere and hydrosphere preferentially enriched in heavy  $^{13}\text{C}$  (Kump and Arthur, 1999; Saltzman and Thomas, 2012). These appear to be global phenomena. For example, the Hirnantian carbon isotope excursion (HICE) of the uppermost Ordovician has been recognized in the western United States (Saltzman, 2005), eastern United States (Bergström et al., 2006), Anticosti Island (Long, 1993), the Baltic Region (Schmitz and Bergström, 2007), the United Kingdom (Underwood et al., 1997), and China (Wang et al., 1997; Fan et al., 2009).

Given the widespread distribution and highly isochronous nature of these signals, they have been employed for chronostratigraphy in sections where biostratigraphical data are

limited (Cramer et al., 2006; McLaughlin et al., 2012a, 2013; Sullivan et al., 2016). Globally recognized patterns have recently been used to create generalized  $\delta^{13}\text{C}$  curves that are integrated with the geological timescale (Fig. 1; Bergström et al., 2009; Cramer et al., 2011; Saltzman and Thomas, 2012). Application of new tools such as these has revolutionized Palaeozoic chronostratigraphy, permitting the calibration of global events and correlations with unprecedented resolution (Cramer et al., 2010, 2015). However, much of this prior work was limited to inorganic  $\delta^{13}\text{C}_{\text{carb}}$  data derived from carbonates, largely confining the application of this method to calcareous rocks.

Although there are studies characterizing  $\delta^{13}\text{C}_{\text{org}}$  in Ordovician to Silurian strata (e.g. Underwood et al., 1997; Cramer and Saltzman, 2007b; Cramer et al., 2010; Edwards and Saltzman, 2015; Loydell et al. 2015) these are mostly confined to the Sheinwoodian or earlier (Kump and Arthur, 1999; Porębska et al. 2004; Cramer and Saltzman, 2005; Melchin and Holmden 2006; Cramer et al. 2010; Gouldey et al. 2010). The organic carbon isotope record for Baltica is particularly limited. A few studies, including the work of Porębska et al. (2004), offer a tantalizing look at the dynamics of these geochemical proxies, albeit through a narrow stratigraphical interval with few samples.

This study presents a large geochemical dataset for two boreholes spanning the Upper Ordovician to upper Silurian in central Poland, representing distal equivalents of well-studied sections in the Baltic Region and western Ukraine (Fig. 2). This dataset is integrated with high-resolution graptolite and palynomorph biostratigraphic data to constrain the age of features identified in these curves. The large body of inorganic geochemistry data also presented here is

also used to characterize depositional environments and seawater chemistry through this turbulent interval of the planet's history.

## 2. Geologic setting

During the mid-Silurian, our study area was situated between 10° and 20° South paleolatitude in southern Baltica (Torsvik and Cocks, 2013). Distinct facies belts traced from Gotland to Podolia have been used to infer proximal-to-basinal depositional environments and the margin of the ancient palaeocontinent (Fig. 2; Einasto et al., 1986; Teller, 1997). The two sections studied here represent deep-water environments in the Lublin basin what is now central Poland (Fig. 2; Teller, 1997; Kiersnowski and Dyrka, 2013).

Although detailed lithostratigraphic interpretation is beyond the scope of this study, the Ordovician strata examined here are likely equivalent to Katian mudstones of the Sasino Formation and uppermost Ordovician calcareous beds assigned to the Prabuty Formation; these are unconformably overlain by Llandovery shales of the Pasłek Formation (Podhalańska, 2007). These in turn are succeeded by thick Wenlock and Ludlow clastics of the Pelplin or Kociewie formations (Modliński and Podhalańska, 2010; see also Szymański and Modliński, 2003).

Strata in the subsurface of Poland have been surveyed in detail by petroleum exploration companies (see summary by Kiersnowski and Dyrka, 2013). Although data from many of these sections remain proprietary, our results benefit from the context established by published geochemical and biostratigraphic work from the boreholes Bartoszyce IG-1 (Porębska

et al., 2004), Widowo IG-1 (Jarochowska and Munnecke, 2015), Wilków-1 (Smolarek et al., 2017), and upper Silurian deposits at Mielnik IG-1 (Kozłowski and Sobieć, 2012).

Although not technically situated within Baltica, coeval strata that crop out in the Holy Cross Mountains may also provide useful stratigraphical context for deep-water depositional environments of the region (Fig. 2; Kozłowski and Munnecke, 2010; Kozłowski et al., 2004; 2014; Smolarek et al., 2017). This area comprises two distinct terranes, Łysogóry in the north and Małopolska in the south, which are situated along the Trans-European Suture Zone (Kozłowski et al., 2014).

The upper Darriwilian, Sandbian, and lower Katian stages in these well-studied sections are represented by a facies mosaic of carbonates, fine- to medium-grained clastics, and phosphatic strata that record complex palaeobathymetry and shifting currents associated with the Late Ordovician convergence of Avalonia and Baltica (Trela, 2005, 2008). The Hirnantian interval here is generally calcareous, comprising argillaceous limestones and marls spanning the *mucronata* trilobite Biozone and *persculptus* graptolite Biozone (Masiak et al., 2003).

The lowermost Silurian in the Holy Cross Mountains consists of organic-rich graptolitic shales and cherts, which are particularly characteristic of the Rhuddanian (Masiak et al., 2003; Smolarek et al., 2017). This interval is also highly condensed compared to the overlying green-grey mudstones of the Aeronian and Telychian (Smolarek et al., 2017). A thicker section of organic-rich beds occurs in the Sheinwoodian *murchisoni*, *riccartonensis* and *flexilis* graptolite biozones; these are also enriched in redox-sensitive trace metals such as V, Mo, and U, suggesting seafloor anoxia and euxinia; uppermost Sheinwoodian strata are less organic-rich, becoming intermittently calcareous in the Homerian (Smolarek et al., 2017). They are overlain

by a thick, coarse clastic interval of greywacke, assumed to derive from a volcanic arc developed on the eastern margin of Avalonia during the final oblique closure of the southern part of the Törnquist Sea (Kozłowski et al., 2004; 2014). These thick, upper Silurian clastic deposits also have spatially complex relationships, controlled by proximity to sediment source and sea-level fluctuations (Kozłowski, 2008).

Graptolites are the primary basis for fine-scale biostratigraphical correlation within the complex geology of Poland's subsurface (e.g. Tomczykowa and Tomczyk, 1979; Masiak et al., 2003), although palynomorphs may be applied here as well (Masiak et al., 2003; Porębska et al., 2004). In more proximal calcareous facies, conodonts have been used (Männik and Małkowski, 1998).

Carbon isotope studies have led to the identification of the positive excursions associated with the upper Homeric Mulde Event in the Widowo IG-1 borehole (Jarochowska and Munnecke, 2015) and at Bartoszyce IG-1, where a positive shift in isotopes is reported in both  $\delta^{13}\text{C}_{\text{carb}}$  and  $\delta^{13}\text{C}_{\text{org}}$  records (Porębska et al., 2004). The large positive excursion associated with the Ludfordian Lau Event has also been identified in Poland at Mielnik IG-1 representing distal regions of Baltica (Kozłowski and Sobieć, 2012) and in the Holy Cross Mountains, where it is found in the Bełcz Member of the Winnica Formation (Kozłowski and Munnecke, 2010).

Older strata have not received the same amount of attention bestowed on well-constrained sections in Ukraine (Kaljo et al., 2007), Lithuania (Kaljo et al., 1998), Estonia (Cramer et al., 2010; Munnecke and Männik, 2009), and Gotland (Bickert et al., 1997; Samtleben et al., 2000; Munnecke et al., 2003; Calner et al., 2004). The elemental geochemistry and stable isotope data from Grabowiec-6 and Zwierzyniec-1 offer a new opportunity to

understand Silurian oceanographic events in deep-water settings and to elucidate the depositional history of these regions of Poland.

### 3. Methods and materials

#### 3.1 Organic carbon isotopes

The sampled part of the Grabowiec-6 section encompasses the Telychian to the Ludlow. A total of 171 samples spanning 598 m was analyzed (Fig. 3): material from below 3640 m represents a cored interval; above this, the samples were cuttings. The Zwierzyniec-1 sampled section ranges from Sadbian through to at least the Gorstian strata; here, 219 samples from core spanning 256 m were analyzed (Fig. 4).

This study employed the technique of Elemental Analyzer - Isotope Ratio Mass Spectrometry (EA-IRMS). Carbonate was removed from rock samples using a solution of hydrochloric acid. Stable isotope ratios from geological samples and internal reference material were measured using a Faraday cup collector array. Internal reference materials include wheat flour ( $\delta^{13}\text{C}_{\text{VPDB}} = -26.43 \text{ ‰}$ ), beet sugar ( $\delta^{13}\text{C}_{\text{VPDB}} = -26.03 \text{ ‰}$ ), and cane sugar ( $\delta^{13}\text{C}_{\text{VPDB}} = -11.64 \text{ ‰}$ ), which are calibrated against IAEA-CH-6 (sucrose,  $\delta^{13}\text{C}_{\text{VPDB}} = -26.03 \text{ ‰}$ ) an inter-laboratory comparison standard distributed by the International Atomic Energy Agency. Values were normalized to the Vienna Peedee Belemnite (VPDB). An approximate total organic carbon (TOC)

value was also produced from this process based on the strength of the ion beam and weight loss from combustion.

### **3.2 Inorganic geochemistry**

Elemental geochemistry samples were powdered and taken into solution, which was then transferred to a fine aerosol and ionized into an inductively coupled plasma (ICP). This material was then analyzed using two methodologies: inductively coupled plasma optical emission spectroscopy (ICP-OES) and inductively coupled plasma mass spectrometry (ICP-MS). Both instruments can acquire abundance data for many of the elements in the periodic table, although when dealing with geological materials, they are best used in combination. Optical emission spectroscopy is most suited to the analysis of major elements and high abundance trace elements (as well as selected low abundance trace elements that are devoid of spectral interferences). On the other hand, mass spectrometry is more suited to the analysis of low abundance trace elements and rare earth elements (REEs).

The analytical methods employed here generated data for the major elements, reported here as their dominant oxides ( $\text{Al}_2\text{O}_3$ ,  $\text{SiO}_2$ ,  $\text{TiO}_2$ ,  $\text{Fe}_2\text{O}_3$ ,  $\text{MnO}$ ,  $\text{MgO}$ ,  $\text{CaO}$ ,  $\text{Na}_2\text{O}$ ,  $\text{K}_2\text{O}$ ,  $\text{P}_2\text{O}_5$ ), trace elements (Ba, Be, Co, Cr, Cs, Cu, Ga, Hf, Nb, Ni, Pb, Rb, Sc, Sn, Sr, Ta, Th, Tl, U, V, W, Y, Zn, Zr) and fourteen rare earth elements (La, Ce, Pr, Nd, Sm, Nd, Gd, Tb, Ho, Dy, Er, Tm, Yb and Lu). Abundance data from several elements were acquired by both ICP-MS and ICP-OES. In the final analyses presented here, abundance data for the major oxides, Ba, Cr, S, Sc, Sr, Zn, and Zr were

generally acquired from ICP-OES measurements, while the remaining elemental results were derived from ICP-MS results.

The oceanographic and depositional significance of results has been inferred based on secular variation in chemostratigraphic curves. However, we have also performed multivariate analysis in the program R (version 3.1.1) to assess overarching patterns of element concentration. For this analysis, the full geochemistry dataset was normalized and the strength of element-pair correlations, measured by Euclidean distance, were summarized in a distance matrix. Hierarchical cluster analysis was then performed on the distance matrix according to Ward's method ("ward.D"). The findings are plotted as dendrograms.

## 4. Results

### 4.1 Biostratigraphy

A large biostratigraphic data set has been generated from graptolites (Appendix A) and palynomorphs (Appendix B, C) collected from the two cores sampled here. The lowest samples from the Grabowiec-6 borehole were recovered at 3815 m (Fig. 3). These comparatively oxic, bioturbated calcareous mudstones yielded few zonal graptolites but many acritarchs and chitinozoans. Specimens from the base of the section up to 3794 m suggest the Upper Ordovician Katian Stage. Diagnostic specimens include the chitinozoans *Belonechitina hirsuta* and *Lagenochitina baltica*. Although less definitive, the low-diversity graptolite assemblage

dominated by *Normalograptus*, but including rare specimens of *Corynoides curtus* and *Lasiograptus harknessi*, is consistent with this age determination.

Higher strata become progressively more calcareous and biomicritic to the top of the Katian. The base of the Silurian is marked by a relatively thin, heavily mineralized zone containing abundant glauconite. The co-occurrence of *Diversograptus ramosus* and *Oktavites spiralis* in dark, organic-rich silty mudstones from 3793.15 m to 3792.81 m indicates a Telychian age (Fig. 3) and the Hirnantian, Rhuddanian, and Aeronian appear to be absent. In higher, brownish-grey, micaceous shales (3787.21-3787.35 m), lower Sheinwoodian *Cyrtograptus murchisoni* Biozone species occur, including *C. murchisoni*, *Monoclimacis kettneri* and *Mediograptus inconspicuus* along with the chitinozoan *Margachitina margaritana* (Fig. 3).

Low-diversity assemblages including the biozonal index species, *Monograptus riccartonensis*, occur between 3785.83 m and 3784.94 m. Higher strata in the core are monotonous, organic-rich, dark-grey, silty mudstones that are sometimes micaceous. Assemblages here include typical later Sheinwoodian graptolites including *Pristiograptus dubius*, *Mediograptus antennularius*, and *Monoclimacis flumendosae*.

The first definitive evidence for the Homeric comes from *Cyrtograptus radians* (in the 3759.89–3760.0 m sample) followed by the biozonal index *Cy. lundgreni* at 3749.95–3750.0 m. *Gothograptus nassa* and diminutive forms of *P. dubius* (often referred to *P. parvus*) occur at 3737.06–3737.10 m, an impoverished assemblage typical of the *nassa* Biozone. Both *Colonograptus deubeli* and *Co. praedeubeli* occur from 3732.40 m to 3732.50 m providing excellent evidence for the Homeric *praedeubeli-deubeli* Biozone. *Colonograptus ludensis*, index species for the uppermost Homeric graptolite biozone, occurs at 3729.8–3730.0 m.

Lower Ludlow taxa, including *Saetograptus* spp. and *Bohemograptus bohemicus* appear at 3728.55 m and the highest core sample examined, from 3644.00-3644.20 m, included the Gorstian graptolite *Lobograptus scanicus*, indicating an expanded Ludlow sequence by comparison with lower parts of the Silurian. These facies are significantly coarser and siltier than underlying Wenlock strata.

To the southwest at Zwierzyniec-1, the lowest core sample processed for palynomorphs was from a depth of 3064.94 m, which yielded the chitinozoan *Spinachitina multiradiata*, indicative of the upper Sandbian Stage of the Upper Ordovician (Fig. 4). A higher sample at 3059.88 m with a single specimen of *Kalochitina multispinata*, suggests possible assignment to the lower Katian Stage (Vandenbroucke et al., 2009). Chitinozoans and acritarchs are rare in overlying samples, although forms attributed to the *Belonechitina hirsuta* complex were observed in the 3044-3025 m interval, indicating a mid-Katian age. This agrees with the graptolite records: the lower Katian biozonal index *Dicranograptus clingani* was found in the 3052.16-3052.25 m sample and the lower to middle Katian *Corynoides ultimus* from 3019.75-3020.0 m. At 3018 m, *Appendispinograptus supernus* and '*Climacograptus*' *latus* indicate the upper Katian (Fig. 4). This is corroborated by the occurrence of the chitinozoan *Lagenochitina baltica* at 3020 m. Like coeval strata at Grabowiec-6, Sandbian and Katian strata here appear to be oxidized and bioturbated.

Unlike Grabowiec-6, evidence for the Hirnantian Stage is present in Zwierzyniec-1; at 3013.97 m the appearance of *Metabolograptus parvulus* with an almost complete median septum, suggests a level low in the *Me. persculptus* Biozone. Hirnantian strata here are

calcareous up to about 2995 m, where clastic content significantly increases and remains high up to organic-rich facies (dark-grey graptolitic mudstones) beginning near 2985 m.

*Me. parvulus* occurs again in the 2985.20-2985.24 m sample, but with a delayed origin of the median septum indicative of a level between the middle *Me. persculptus* Biozone and middle *Akidograptus ascensus-Parakidograptus acuminatus* Biozone. The biozonal index *Ak. ascensus* appears at 2984.0 m with the mid *ascensus-acuminatus* Biozone indicator *Normalograptus trifilis* at 2981.97 m. The presence of *Rhaphidograptus extenuatus* at 2978.88 m indicates the middle Rhuddanian *Cystograptus vesiculosus* Biozone. Three core samples of dark-grey laminated mudstones (2970.31-2970.42 m, 2971.63-2971.73 m and 2974.50-2974.63 m) can be assigned to the upper Rhuddanian *Pernerograptus revolutus* Biozone. Biostratigraphically important species present include *Cystograptus penna*, *C. vesiculosus*, *Pe. revolutus*, *Pseudorthograptus mutabilis*, *Ps. obuti* and *Dimorphograptus swanstoni*.

Between 2970 m and 2969 m there are abundant slickensides and quartz veining, and the lower Aeronian *triangulatus* and *magnus* biozones appear to be absent. Core of dark grey mudstones and shales from between 2969.00 m and 2969.35 m contain high-diversity graptolite assemblages typical of the Aeronian *Pribylograptus leptotheca* Biozone. Species present include *Petalolithus praecursor*, *Campograptus lobiferus*, *Coronograptus maxiculus*, *Lituigraptus richteri* and '*Monograptus*' *inopinus*. Overlying this is a thin interval (up to 2968 m) containing upper *leptotheca* or possibly lower *convolutus* Biozone graptolites.

Between 2968 m and 2952.95 m the pale burrowed mudrocks present did not yield graptolites. A level in the upper *spiralis* Biozone is indicated by *Stimulograptus vesiculosus* in dark silty mudstones at 2952.95 m with a lower *Cyrtograptus lapworthi* Biozone assemblage

occurring in grey micaceous mudstones at 2951.32-2951.48 m, including *Streptograptus wimani*, *Oktavites spiralis* and *Barrandeograptus pulchellus*. Only 1.32 m higher in the core (2949-2950 m samples) significantly younger graptolites occur in brownish grey micaceous shales, including *C. murchisoni* and *Mediograptus inconspicuus*, which characteristic of the lower Sheinwoodian *Cyrtograptus murchisoni* Biozone.

*Cyrtograptus murchisoni* occurs up to the 2941.49-2941.92 m sample, above which, up to 2938.70 m *Monograptus riccartonensis* was recorded. Typical upper Sheinwoodian assemblages, including the biozonal index species *Cyrtograptus rigidus*, were recorded from dark grey silty mudstones between 2935.10 m and 2925.30 m. Above this, the interval from 2921.07 m to 2872.90 m can be assigned to the lower Homerian, with assemblages including the biozonal index *Cyrtograptus lundgreni*. The first evidence for the Gorstian in the siltier faces of the upper core is from 2825.0-2825.2 m with the first appearances of *Bohemograptus bohemicus* and *Spinograptus spinosus*.

#### 4.2. Stable carbon isotopes

A total of 345 new  $\delta^{13}\text{C}_{\text{org}}$  data points have been generated for this study (Appendix D). The 126 samples from Grabowiec-6 have a mean of  $-29.2\text{‰}$ , a median of  $-29.3\text{‰}$ , and a standard deviation of  $1.1\text{‰}$ . Isotopically heavy values (over  $-29.5\text{‰}$ ) are found in the Telychian to lower Sheinwoodian strata near the bottom of our measured section. They drop significantly through higher Sheinwoodian strata to a minimum of almost  $-32\text{‰}$  in the lower Homerian before rising with the appearance of *Cyrtograptus lundgreni* (Fig. 3). Values reach

another local peak at  $-28.8$  ‰ in the *nassa* to *ludensis* interval (3732 m). Carbon isotope values at Grabowiec-6 then fluctuate between  $-31.0$  ‰ and  $-27.9$  ‰ through the Gorstian, although they rise about 1 ‰ overall through the next 100 m of strata before a sharp peak value of  $-25.8$  ‰ at 3618 m. Values drop back to below  $-29.0$  ‰ in the 20 m above this, where we reach the top of our measured section.

The 219 samples from Zwierzyniec-1 have a mean value of  $-30.1$  ‰, a median of  $-30.3$  ‰, and a standard deviation of 1.1 ‰. Sandbian strata at the base of our measured section have relatively high  $\delta^{13}\text{C}_{\text{org}}$  values above  $-30.0$  ‰, which drop by almost 1 ‰ at the base of the Katian. Values remain low (between  $-31.2$  ‰ and  $-28.8$  ‰) through the Katian into the lower Hirnantian. However, at 3004 m values rise sharply to a peak at  $-27.0$  ‰ coincident with calcareous Hirnantian strata. Above the overlying sample gap (the Rhuddanian *vesiculosus* to *revolutus* interval), values are at their lowest in the entire section ( $-33.9$  ‰). Values rise again up to another positive excursion in the lower Sheinwoodian, peaking at about  $-28.0$  ‰ in the *riccartonensis* Biozone before declining upward to a minimum at the top of the *rigidus* Biozone. Above this, values range from  $-31.5$  ‰ to  $-29.3$  ‰ through the Homerian and Gorstian. Although there is a lot of scatter, values generally rise by about 1 ‰ through the upper 100 m of measured section.

#### **4.3 Elemental geochemistry**

A total of 67 samples from Grabowiec-6 and 262 samples from Zwierzyniec-1 were analyzed for inorganic geochemistry using ICP analysis (Appendix E). To confirm depth control,

results from three radiogenic elements (Th, U, and  $K_2O$ ) were plotted against the gamma logs (Figs. 3, 4). Overall these curves tended to move in lock-step.

In both sections,  $SiO_2$  is the dominant inorganic component with a mean value of 53.9 wt. % over the entire dataset. High levels of  $Al_2O_3$  (mean = 14.0 wt. %) characterize these sections as well, and this element is positively correlated with  $SiO_2$ . CaO is locally abundant, particularly in Hirnantian strata at Zwierzyniec-1, where it may comprise up to 31.8 wt. % of a sample; this element is negatively correlated with both  $Al_2O_3$  and  $SiO_2$ .

To investigate overarching lithological, depositional, and diagenetic controls on the concentrations of different elements, we have run a one-way hierarchical cluster analysis on the dataset from Grabowiec-6 (Fig. 5) and Zwierzyniec-1 (Fig. 6). For the purposes of discussion, we have labelled major branches for certain representative elements. Although there are strong similarities in element behavior between the different sections, one notable difference is the rare earth elements which cluster with the CaO-MnO group and  $Fe_2O_3$ -S group at Grabowiec-6 (Fig. 5) but with the  $Al_2O_3$ - $TiO_2$ - $SiO_2$  group at Zwierzyniec-1 (Fig. 6).

Selected geochemical profiles that may have chemostratigraphic value or could offer insight to changing depositional and oceanographic processes have been plotted (Fig. 7). The  $SiO_2 / Zr$  ratio is generally high through the Katian-to-Rhuddanian interval of Zwierzyniec-1. In both sections, it is lower through the Aeronian-to-lower-Sheinwoodian interval before rising to a local high in the mid-to-upper Sheinwoodian. From here values remain relatively high through the upper Homeric and Gorstian.  $TiO_2 / Al_2O_3$  ratios are low in the Katian at Zwierzyniec-1 but rise in the Hirnantian and stay high into the lower Homeric. Likewise, relatively high  $TiO_2 / Al_2O_3$

values are observed through the Telychian and Sheinwoodian at Grabowiec-6. Although they decline in the upper Silurian, they do not do so until the top of the Homerician at this section.

Various redox sensitive heavy metals have slightly different behaviors. Some, like Co, Fe<sub>2</sub>O<sub>3</sub>, Ni, and V have distinct peaks in strata that immediately underlie or are coeval to positive carbon isotope excursions, particularly at Zwierzyniec-1 (Fig. 7). Ni, V and Mo are significantly enriched in Sheinwoodian to Homerician strata above these carbon isotope excursions.

A significant enrichment of these trace metals, along with many rare earth elements was also observed at Zwierzyniec-1, centered on 2969 m (Fig. 7). This coincides with a heavily mineralized, deformed zone containing many slickensides.

## 5. Discussion

The Silurian composite curve of Cramer et al. (2011) is based primarily on  $\delta^{13}\text{C}_{\text{carb}}$  data which dominate the published carbon isotope records from Baltica and Laurentia. Paired  $\delta^{13}\text{C}_{\text{carb}}$  and  $\delta^{13}\text{C}_{\text{org}}$  curves have been published for many localities on various palaeocontinents enabling comparisons to be made of individual sections (e. g. Porębska et al., 2004; Noble et al., 2005; Melchin and Holmden, 2006; Cramer and Saltzman, 2007; Cramer et al., 2010; Gouldey et al., 2010; Racki et al., 2012). In some cases, the  $\delta^{13}\text{C}_{\text{carb}}$  and  $\delta^{13}\text{C}_{\text{org}}$  curves show broadly parallel trends and a correlation between datasets can be attempted (Fig. 8). Similar relationships are also seen in the Banwy River section Wales (Cramer et al. 2010), the Wenlock of Arctic Canada (Noble et al., 2005), and Homerician of Poland (Porębska et al., 2004) in all of which major positive excursions recognized in the  $\delta^{13}\text{C}_{\text{carb}}$  record are clearly discernible in organic carbon

records as well. However, in a few other localities, such as the Newsom roadcut, Nashville, Tennessee,  $\delta^{13}\text{C}_{\text{org}}$  values show slightly different patterns from those seen in  $\delta^{13}\text{C}_{\text{carb}}$  data (Cramer and Saltzman, 2007).

Certain key features of the composite curve are readily apparent in our  $\delta^{13}\text{C}_{\text{org}}$  data. The Hirnantian positive isotope excursion (HICE) can be recognized in Zwierzyniec-1, between depths of 2985 m and 3005 m within the upper Hirnantian *Metabolograptus persculptus* Biozone (Fig. 4). Above the HICE in Rhuddanian strata, values have shifted strongly to the negative, which parallels observations at Dob's Linn, Scotland (Underwood et al., 1997), the Canadian Arctic (Melchin and Holmden, 2006), and South China (Yan et al., 2009).

Carbon isotope data is inconsistent through the Llandovery, but much insight can be gained from the distribution of taxa and facies. At Zwierzyniec-1, the sharp boundary between the *vesiculosus* to *revolutus* biozones and the *leptotheca* to *convolutes* biozones at 2970 m suggests a major chronostratigraphic gap. The heavily mineralized zone straddling this level contains many slickensides and deformed beds, suggesting that a fault has removed much of the record.

A very narrow stratigraphic interval (1.3 m) also separates the upper Telychian *lapworthi* Biozone from the Sheinwoodian *murchisoni* Biozone at Zwierzyniec-1 as well. Although this could suggest another fault, it may represent a highly condensed upper Telychian sequence in the section or, more probably an unconformity at this level, such as is seen in sections in the East Baltic region (Loydell et al., 2003, 2010), where all or part of the upper *lapworthi*, *insectus* and *centrifugus* biozones are commonly missing.

The *Cyrtograptus purchisoni* Biozone and the lower Sheinwoodian (Ireviken) positive isotope excursion can be correlated between the Zwierzyniec-1 and Grabowiec-6 wells (Fig. 7). In Grabowiec-6, *murchisoni* Biozone graptolites occur at 3787.21–3781.35 m and this level is immediately succeeded by a positive  $\delta^{13}\text{C}_{\text{org}}$  excursion which has its peak value within the *riccartonensis* Biozone, as it does also in Zwierzyniec-1.

Another, less pronounced excursion occurs higher in the Grabowiec-6 section, commencing around 3750 m and reaching values of  $-29.0\text{‰}$ . Identification of the *praedeubeli/deubeli* Biozone at 3732.40–3732.50 m indicates that this is probably the Homeric Mulde positive isotope excursion. Although lower Homeric graptolites were observed from Zwierzyniec-1, none was identified from the *praedeubeli-deubeli* and *ludensis* biozones and no unambiguous positive carbon isotope shift could be confidently interpreted as the excursion.

The most positive values in the Grabowiec-6 section occur around 3618 m. With a Gorstian graptolite assemblage including *Lobograptus scanicus* occurring at 3644.00–3644.20 m, this feature must represent a post-Wenlock event. Considering its magnitude, it might be envisaged to represent the mid-Ludfordian Lau Excursion. This, however, would suggest a much thinner sequence of Ludlow strata in the Grabowiec-6 well than is typical for this part of Poland (e.g. Jaworowski, 2000). It is likely that it represents the lower Ludfordian excursion sometimes observed in the *Sa. leintwardinensis* graptolite Biozone (Fig. 1; Cramer et al., 2011). This feature is seen at many localities in central and eastern Europe through an interval bearing *Pseudomonoclimacis dalejensis* (junior synonym = *Ps. tauragensis*), a species with a stratigraphical range encompassing the early Ludfordian *leintwardinensis* graptolite extinction

event (Fig. 8; Martma et al., 2005; Štorch et al., 2014) which occurred at the end of the *leintwardinensis* Zone.

Elemental geochemistry data may provide some insight to the depositional and environmental conditions that prevailed in these deep-water depositional environments of the Ordovician and Silurian. Selected element abundances and ratios have been plotted with the new carbon isotope data; these curves have been filled above or below certain values to highlight interesting trends (Fig. 7).

Although detailed sedimentological and mineralogical analyses are beyond the scope of this study, some general interpretations may be drawn from statistical analyses of our geochemical data and the results of earlier workers. We have inferred the possible genetic significance of the larger element groups that emerge from a hierarchical cluster analysis (Fig. 5, 6), further informed by the known mineralogical affinities of various elements.

Predominantly clastic strata from Zwierzyniec-1 and Grabowiec-6 are chemically similar in many respects. In both,  $\text{SiO}_2$  is the dominant inorganic component; and its correlation with  $\text{Al}_2\text{O}_3$  suggests a detrital control on both. A negative correlation of both elements with CaO suggests that this element approximates carbonate content in these rocks, an inference supported by high CaO peaks coincident with calcareous zones (Fig. 7).

There are broad similarities in the clustering of elements in both sections. However, one major discrepancy is the affinity of the rare earth elements, which have a stronger correlation to lithogenic elements in Zwierzyniec-1 (Fig. 6). This appears to be driven by anomalous data from a thin, metalliferous interval close to the Rhuddanian-Aeronian boundary (2970 m), which

was interpreted as a fault (Fig. 4). The unusual chemistry of samples through this interval may be related to hydrothermal enrichment of certain metals along the fault (Fig. 7).

Different ratios and other trace elements may offer some insight to depositional history. Given that sedimentary Zr is almost exclusively found in detrital zircon, the  $\text{SiO}_2 / \text{Zr}$  ratios shown here represent the “excess” silica present in each sample that is likely accounted for via non-detrital sources (Ratcliffe et al., 2012). High values in the Rhuddanian at Zwierzyniec-1 may have a genetic link with the basal Silurian cherts seen in the Holy Cross Mountains.

The  $\text{TiO}_2 / \text{Al}_2\text{O}_3$  ratio may have some value for chemostratigraphic correlation and could also shed light on sediment provenance. An influx of sediment from more mafic source rocks can be manifested as an enrichment of  $\text{TiO}_2$  in relation to  $\text{Al}_2\text{O}_3$  in earlier studies of clastic successions (Girty et al., 1996). A shift to lower  $\text{TiO}_2 / \text{Al}_2\text{O}_3$  in the upper Silurian at both borehole localities could reflect a shift to more felsic provenance, although it is difficult to control for the influence of grain-size in these coarsening-upward sections.

Redox-sensitive trace elements such as Co, Cu, Ni, Mo, V, and Zn are often enriched in sediments that were deposited under low oxygen conditions, and in organic matter as well (Tribovillard et al., 2006). The relative abundance of these may be of some use for understanding oceanographic conditions surrounding the positive  $\delta^{13}\text{C}_{\text{org}}$  excursions in Grabowiec-6 and Zwierzyniec-1 (Fig. 7). V and Mo are particularly enriched in strata deposited above the Sheinwoodian Ireviken Excursion in both Grabowiec-6 and Zwierzyniec-1. In addition to its potential utility for chemostratigraphic correlation, these metals are particularly indicative of anoxic to euxinic conditions (Tribovillard et al., 2006). Elevated values for both, which continue well into the Homeric, could indicate that persistent low-oxygen (potentially sulfidic)

conditions occurred in deep-water settings for a long period after the excursion had subsided (Tribovillard et al., 2006; Smolarek et al., 2017).

Stratigraphically thinner spikes in the concentration of V, Ni, Pb, and Fe<sub>2</sub>O<sub>3</sub> occur in lower Hirnantian strata in Zwierzyniec-1 just below the HICE. Enrichments of Pb and Fe<sub>2</sub>O<sub>3</sub> also occur below the lower Sheinwoodian Ireviken Excursion, but not at the same level. Fe<sub>2</sub>O<sub>3</sub> appears to peak in the Telychian, while Pb does at the base of the Sheinwoodian in both Grabowiec-6 and Zwierzyniec-1.

Some of these elements may also have some relation to redox conditions but the fact that there is no significant enrichment in Pb and Fe<sub>2</sub>O<sub>3</sub> in the wake of the Ireviken Excursion may suggest a more complex history of seawater chemistry. It is possible that these signals may also be linked with the occurrence of malformed phytoplankton during early Paleozoic bioevents reported in some studies (Munnecke et al., 2012). These authors have suggested that high levels of dissolved heavy metals in the water column, including Fe<sub>2</sub>O<sub>3</sub> and Pb, may be linked to the teratological assemblages (Vandenbroucke et al., 2015). This is thought to have been driven by persistent anoxia in the deep sea and remobilization of redox sensitive elements (Emsbo et al., 2010; McLaughlin et al., 2012a). However, concentration of these elements in the substrate requires oxidizing conditions, pointing to intermittent oxidation of the shelf during the event, as suggested by Smolarek et al. (2017). Although some uncertainty continues to surround the ultimate driving forces of these early Silurian palaeoceanographic events, these data may at the least shed some light on their manifestation in deep-water settings in Baltica.

## 8. Conclusions

These new data permit the characterization of new geochemical datasets in biostratigraphically well-constrained distal facies in central Poland. Globally recognized positive shifts have been recognized, including the HICE, the lower Sheinwoodian (Ireviken), Homerian (Mulde) and lower Ludfordian excursions. Redox sensitive trace elements V, Mo, and Ni are significantly enriched in strata above the Ireviken Excursion at both Grabowiec-6 and Zwierzyniec-1 suggesting persistent anoxic to sulfidic deep-water environments in the wake of the event. Stratigraphically narrower spikes of Ni, Pb, and  $\text{Fe}_2\text{O}_3$  below and concurrent with positive excursions here may offer some insight to the oceanographic conditions during the event and may be linked to the abundant, malformed palynomorphs observed in coeval sections.

The results discussed here also provide the groundwork for future studies of carbon isotopes through strata where  $\delta^{13}\text{C}_{\text{carb}}$  data are limited by the absence of carbonate. Furthermore, they may also help begin to elucidate the high-resolution chronostratigraphical relationships of Silurian bedrock in the deep subsurface of east-central Europe and the conditions leading up to major Silurian palaeoceanographic events.

### **Acknowledgements**

We thank Emilia Jarachowska and Wojciech Kozłowski for critical reviews that greatly strengthened the content of this manuscript. We also thank Chevron Corporation for permission to share the results described here. New elemental geochemistry data here were

generated by the labs at Chemostrat Ltd. Stable isotope data were provided by ISO-Analytical Ltd. Palynological samples were prepared in the Palynology Laboratory of the British Geological Survey, Keyworth, Nottingham, U.K., by Mrs. J. Flint. Stewart G. Molyneux publishes by permission of the Executive Director, British Geological Survey (NERC). Nicholas B. Sullivan acknowledges support from Chemostrat Inc.

ACCEPTED MANUSCRIPT

## References

- Aldridge, R.J., Jeppsson, L., Dorning, K.J., 1993. Early Silurian oceanic episodes and events. *Journal of the Geological Society, London* 150, 501-513.
- Bergström, S.M., Chen, X., Gutiérrez-Marco, J.C., Dronov, A., 2009. The new chronostratigraphic classification of the Ordovician System and its relations to major regional series and stages and to  $\delta^{13}\text{C}$  chemostratigraphy. *Lethaia* 42, 97-107.
- Bergström, S.M., Saltzman, M.M., Schmitz, B., 2006. First record of the Hirnantian (Upper Ordovician)  $\delta^{13}\text{C}$  excursion in the North American Midcontinent and its regional implications. *Geological Magazine* 143, 657-678.
- Bickert, T., Pätzold, J., Samtleben, C., Munnecke, A., 1997. Paleoenvironmental changes in the Silurian indicated by stable isotopes in brachiopod shells from Gotland, Sweden. *Geochimica et Cosmochimica Acta* 61, 2717-2730.
- Calner, M., Jeppsson, L., Munnecke, A., 2004. The Silurian of Gotland—Part I: review of the stratigraphic framework, event stratigraphy, and stable carbon and oxygen isotope development. *Erlanger geologische Abhandlungen, Sonderband* 5, 113-131.
- Cramer, B.D., Brett, C.E., Melchin, M.J., Männik, P., Kleffner, M.A., McLaughlin, P.I., Loydell, D.K., Munnecke, A., Jeppsson, L., Corradini, C., Brunton, F.R., 2011. Revised correlation of Silurian Provincial Series of North America with global and regional chronostratigraphic units and  $\delta^{13}\text{C}_{\text{carb}}$  chemostratigraphy. *Lethaia* 44, 185–202.
- Cramer, B.D., Kleffner, M.A., Saltzman, M.R., 2006. The late Wenlock Mulde positive carbon isotope ( $\delta^{13}\text{C}_{\text{carb}}$ ) excursion in North America. *GFF* 128, 85-90.

- Cramer, B.D., Loydell, D.K., Samtleben, C., Munnecke, A., Kaljo, D., Männik, P., Martma, T., Jeppsson, L., Kleffner, M.A., Barrick, J.E., Johnson, C.A., 2010. Testing the limits of Paleozoic chronostratigraphic correlation via high-resolution (< 500 ky) integrated conodont, graptolite, and carbon isotope ( $\delta^{13}\text{C}_{\text{carb}}$ ) biochemostratigraphy across the Llandovery–Wenlock (Silurian) boundary: is a unified Phanerozoic time scale achievable? Geological Society of America Bulletin 122, 1700-1716.
- Cramer, B.D., Munnecke, A., 2008. Early Silurian positive  $\delta^{13}\text{C}$  excursions and their relationship to glaciations, sea-level changes and extinction events: discussion. Geological Journal 43, 517.
- Cramer, B.D., Saltzman, M.R., 2005. Sequestration of  $^{12}\text{C}$  in the deep ocean during the early Wenlock (Silurian) positive carbon isotope excursion. Palaeogeography, Palaeoclimatology, Palaeoecology 219, 333-349.
- Cramer, B.D., Saltzman, M.R., 2007a. Fluctuations in epeiric sea carbonate production during Silurian positive carbon isotope excursions: A review of proposed paleoceanographic models. Palaeogeography, Palaeoclimatology, Palaeoecology 245, 37-45.
- Cramer, B.D., Saltzman, M.R., 2007b. Early Silurian paired  $\delta^{13}\text{C}_{\text{carb}}$  and  $\delta^{13}\text{C}_{\text{org}}$  analyses from the Midcontinent of North America: implications for paleoceanography and paleoclimate. Palaeogeography, Palaeoclimatology, Palaeoecology 256, 195-203.
- Cramer, B.D., Vandenbroucke, T.R., Ludvigson, G.A., 2015. High-Resolution Event Stratigraphy (HiRES) and the quantification of stratigraphic uncertainty: Silurian examples of the quest for precision in stratigraphy. Earth-Science Reviews 141, 136-153.

- Edwards, C.T., Saltzman, M.R., 2015. Paired carbon isotopic analysis of Ordovician bulk carbonate ( $\delta^{13}\text{C}_{\text{carb}}$ ) and organic matter ( $\delta^{13}\text{C}_{\text{org}}$ ) spanning the Great Ordovician Biodiversification Event. *Palaeogeography, Palaeoclimatology, Palaeoecology* 458, 102-117.
- Einasto, R.E., Abushik, A.F., Kaljo, D.L., Koren, T.N., Modzalevskaya, T.L., Nestor, H.E., 1986. Silurian sedimentation and the fauna of the East Baltic and Podolian marginal basins: a comparison. In: Kaljo, D., Klaamann, E. (Eds.), *Theory and Practice of Ecostratigraphy*. Valgus, Tallinn, 65-72, 269.
- Emsbo, P., McLaughlin, P.I., Munnecke, A., Breit, G.N., Koenig, A.E., Jeppsson, L., Verplanck, P.L., 2010. The Ireviken Event: A Silurian OAE. *Geological Society of America Abstracts with Programs* 42(5), 561.
- Fan, J., Peng, P.A., Melchin, M.J., 2009. Carbon isotopes and event stratigraphy near the Ordovician–Silurian boundary, Yichang, South China. *Palaeogeography, Palaeoclimatology, Palaeoecology* 276, 160-169.
- Gouldey, J.C., Saltzman, M.R., Young, S.A., Kaljo, D., 2010. Strontium and carbon isotope stratigraphy of the Silurian (Early Silurian): implications for tectonics and weathering. *Palaeogeography, Palaeoclimatology, Palaeoecology* 296, 264-275.
- Hill, P.J., Dorning, K.J. 1984. Appendix 1: Acritarchs. In: Cocks, L.R.M., Woodcock, N.H., Rickards, R.B., Temple, J.T., Lane, P.D., *The Llandovery Series of the Type Area*. *Bulletin of the British Museum (Natural History), Geology Series* 38, 131-182.

- Jarochowska, E., Munnecke, A., 2015. Late Wenlock carbon isotope excursions and associated conodont fauna in the Podlasie Depression, eastern Poland: a not-so-big crisis? *Geological Journal* 51, 683-703.
- Jeppsson, L., 1993. Silurian events: the theory and the conodonts. *Proceedings of the Estonian Academy of Sciences, Geology*, 42, 23-27.
- Jeppsson, L., 1997a. The anatomy of the mid-early Silurian Ireviken Event and a scenario for PS events. In: Brett, C.E., Baird, G.C. (Eds.), *Paleontological events: stratigraphic, ecological, and evolutionary implications*. Columbia University Press, New York, 451-492.
- Jeppsson, L. 1997b. A new latest Telychian, Sheinwoodian and Early Homerian (Early Silurian) standard conodont zonation. *Transactions of the Royal Society of Edinburgh: Earth Sciences* 88, 91-114.
- Jeppsson, L., 1998. Silurian oceanic events: summary of general characteristics. *New York State Museum Bulletin* 491, 239-257.
- Kaljo, D., Kiipli, T., Martma, T., 1998. Correlation of carbon isotope events and environmental cyclicity in the East Baltic Silurian. *New York State Museum Bulletin* 491, 297-312.
- Kaljo, D., Grytsenko, V., Martma, T., Mõtus, M.A., 2007. Three global carbon isotope shifts in the Silurian of Podolia (Ukraine): stratigraphical implications. *Estonian Journal of Earth Sciences* 56, 205-220.
- Kaljo, D., Kiipli, T., Martma, T., 1997. Carbon isotope event markers through the Wenlock–Přídolí sequence at Ohesaare (Estonia) and Priekule (Latvia). *Palaeogeography, Palaeoclimatology, Palaeoecology* 132, 211-223.

- Kaljo, D. and Martma, T., 2006. Application of carbon isotope stratigraphy to dating the Baltic Silurian rocks. *GFF* 128, 123-129.
- Kiersnowski, H., Dyrka, I., 2013. Ordovician-Silurian shale gas resources potential in Poland: evaluation of Gas Resources Assessment Reports published to date and expected improvements for 2014 forthcoming Assessment. *Przegląd Geologiczny* 61, 354-379.
- Kozłowski, W., 2008. Lithostratigraphy and regional significance of the Nowa Słupa Group (Upper Silurian) of the Łysogóry region (Holy Cross Mountains, central Poland). *Acta Geologica Polonica* 58, 43-74.
- Kozłowski, W., Domańska, J., Nawrocki, J., Pecskay, Z., 2004. The provenance of the upper Silurian greywackes from the Holy Cross Mountains (central Poland). *Mineralogical Society of Poland* 24, 251-254.
- Kozłowski, W., Munnecke, A., 2010. Stable carbon isotope development and sea-level changes during the late Ludlow (Silurian) of the Łysogóry region (Rzepin section, Holy Cross Mountains, Poland). *Facies* 56, 615-633.
- Kozłowski, W., Sobień, K., 2012. Mid-Ludfordian coeval carbon isotope, natural gamma ray and magnetic susceptibility excursions in the Mielnik IG-1 borehole (Eastern Poland)—dustiness as a possible link between global climate and the Silurian carbon isotope record. *Palaeogeography, Palaeoclimatology, Palaeoecology* 339, 74-97.
- Kozłowski, W., Domańska-Siuda, J., Nawrocki, J., 2014. Geochemistry and petrology of the Upper Silurian greywackes from the Holy Cross Mountains (central Poland): implications for the Caledonian history of the southern part of the Trans-European Suture Zone (TESZ). *Geological Quarterly* 58, 311-336.

- Kump, L.R., Arthur, M.A., 1999. Interpreting carbon-isotope excursions: carbonates and organic matter. *Chemical Geology* 161, 181-198.
- Long, D.G., 1993. Oxygen and carbon isotopes and event stratigraphy near the Ordovician—Silurian boundary, Anticosti Island Quebec. *Palaeogeography, Palaeoclimatology, Palaeoecology* 104, 49–59.
- Loydell, D.K., 2007. Early Silurian positive  $\delta^{13}\text{C}$  excursions and their relationship to glaciations, sea-level changes and extinction events. *Geological Journal* 42, 531-546.
- Loydell, D.K., 2008. Reply to 'Early Silurian positive  $\delta^{13}\text{C}$  excursions and their relationship to glaciations, sea-level changes and extinction events: discussion' by Bradley D. Cramer and Axel Munnecke. *Geological Journal* 43, 511-515.
- Loydell, D.K., Frýda, J., 2007. Carbon isotope stratigraphy of the upper Telychian and lower Sheinwoodian (Llandovery–Wenlock, Silurian) of the Banwy River section, Wales. *Geological Magazine* 144, 1015-1019.
- Loydell, D.K., Frýda, J., Gutiérrez-Marco, J.C., 2015. The Aeronian/Telychian (Llandovery, Silurian) boundary, with particular reference to sections around the El Pintado reservoir, Seville Province, Spain. *Bulletin of Geosciences* 90, 743-794.
- Loydell, D.K., Männik, P., Nestor, V., 2003. Integrated biostratigraphy of the lower Silurian of the Aizpute-41 core, Latvia. *Geological Magazine* 140, 205-229.
- Loydell, D.K., Nestor, V., Männik, P., 2010. Integrated biostratigraphy of the lower Silurian of the Kolka-54 core, Latvia. *Geological Magazine* 147, 253-280.
- Männik, P., 2005. Early Telychian Valgu Event—some preliminary data from Estonia. *Evolution of Life on the Earth: Proceedings of the III International Symposium*, 134-137.

- Männik, P., Małkowski, K.C., 1998. Silurian conodonts from the Gołdap core, Poland. *Palaeontologia Polonica* 58, 141-151.
- Männik, P., 2007. An updated Telychian (Late Llandovery, Silurian) conodont zonation based on Baltic faunas. *Lethaia* 40, 45-60.
- Martma, T., Brazauskas, A., Kaljo, D., Kaminskas, D., Musteikis, P., 2005. The Wenlock-Ludlow carbon isotope trend in the Vidukle core, Lithuania, and its relations with oceanic events. *Geological Quarterly* 49, 223-234.
- Masiak, M., Podhalańska, T., Stempień-Safek, M., 2003. Ordovician–Silurian boundary in the Bardo Syncline, Holy Cross Mountains, Poland – new data on fossil assemblages and sedimentary succession. *Geological Quarterly* 47, 311-330.
- McLaughlin, P.I., Emsbo, P., Brett, C.E., 2012a. Beyond black shales: the sedimentary and stable isotope records of oceanic anoxic events in a dominantly oxic basin (Silurian; Appalachian Basin, USA). *Palaeogeography, Palaeoclimatology, Palaeoecology* 367, 153-177.
- McLaughlin, P.I., Emsbo, P., Mikulic, D.G., Brett, C.E., 2012b. Detection of the Lau Excursion across the eastern US—key to regional Silurian chronostratigraphy. In: Cramer, B.D., (Ed.), *Abstracts from the International Geoscience Program (IGCP) Project 591 2nd Annual Meeting and 1st Foerste Symposium, Cincinnati, Ohio*, p. 24.
- McLaughlin, P.I., Mikulic D.G., Kluessendorf J. 2013. Age and correlation of Silurian rocks in Sheboygan, Wisconsin, using integrated stable carbon isotope stratigraphy and facies analysis. *Wisconsin Geoscience* 21, 15-38.

- Melchin, M.J., Holmden, C., 2006. Carbon isotope chemostratigraphy of the Llandovery in Arctic Canada: implications for global correlation and sea-level change. *GFF* 128, 173-180.
- Melchin, M.J., Koren, T.N., Štorch, P., 1998. Global diversity and survivorship patterns of Silurian graptoloids. *New York State Museum Bulletin* 491, 165-182.
- Melchin, M.J., Sadler, P.M., Cramer, B.D., Cooper, R.A., Gradstein, F.M., Hammer, O., 2012. The Silurian Period. In: Gradstein, F.M., Ogg, J.G., Schmitz, M.D., Ogg, G.M. (Eds.), *The Geologic Time Scale 2012, Volume 2*. Elsevier. 525-558.
- Modliński, Z., Podhalańska, T., 2010. Outline of the lithology and depositional features of the lower Paleozoic strata in the Polish part of the Baltic region. *Geology Quarterly* 54(2), 109-121.
- Molyneux, S.G., Le Hérisse, A., Wicander, R., 1996. Chapter 16. Paleozoic phytoplankton. In: Jansonius, J., McGregor, D.C. (Eds.), *Palynology: principles and applications, Volume 2*. American Association of Stratigraphic Palynologists Foundation, 493-529.
- Mullins, G.L., 2001. Acritarchs and prasinophyte algae of the Elton Group, Ludlow Series, of the type area. *Monograph of the Palaeontographical Society, London* 155, 1-151.
- Munnecke, A., Delabroye, A., Servais, T., Vandenbroucke, T.R.A., Vecoli, M., 2012. Systematic occurrences of malformed (teratological) acritarchs in the run-up of Early Palaeozoic  $\delta^{13}\text{C}$  isotope excursions. *Palaeogeography, Palaeoclimatology, Palaeoecology*, 367, 137-146.
- Munnecke, A., Männik, P., 2009. New biostratigraphic and chemostratigraphic data from the Chicotte Formation (Llandovery, Anticosti Island, Laurentia) compared with the Viki core (Estonia, Baltica). *Estonian Journal of Earth Sciences* 58, 159-169.

- Munnecke, A., Samtleben, C., Bickert, T., 2003. The Ireviken Event in the lower Silurian of Gotland, Sweden—relation to similar Palaeozoic and Proterozoic events. *Palaeogeography, Palaeoclimatology, Palaeoecology* 195, 99-124.
- Noble, P.J., Zimmerman, M.K., Holmden, C., Lenz, A.C., 2005. Early Silurian (Wenlockian)  $\delta^{13}\text{C}$  profiles from the Cape Phillips Formation, Arctic Canada and their relation to biotic events. *Canadian Journal of Earth Sciences* 42, 1419-1430.
- Podhalańska, T., 2007. Late Ordovician to Early Silurian transition and the graptolites from Ordovician/Silurian boundary near the SW rim of the East European Craton (northern Poland). Proceedings, 7<sup>th</sup> International Graptolite Conference & Field Meeting, Subcommittee on Silurian Stratigraphy 18, 165-171.
- Porębska, E., Kozłowska-Dawidziuk, A., Masiak, M., 2004. The *lundgreni* event in the Silurian of the East European Platform, Poland. *Palaeogeography, Palaeoclimatology, Palaeoecology* 213, 271-294.
- Racki, G., Balinski, A., Wrona, R., Małkowski, K., Drygant, D., Szaniawski, H., 2012. Faunal dynamics across the Silurian-Devonian positive isotope excursions ( $\delta^{13}\text{C}$ ,  $\delta^{18}\text{O}$ ) in Podolia, Ukraine: Comparative analysis of the Ireviken and Klonk events. *Acta Palaeontologica Polonica* 57, 795-832.
- Ratcliffe, K.T., Wright, A.M., Montgomery, P., Palfrey, A., Vonk, A., Vermeulen, J., Barrett, M., 2010. Application of chemostratigraphy to the Mungaroo Formation, the Gorgon Field, offshore northwest Australia. *APPEA Journal* 2010-50<sup>th</sup> Anniversary Issue, 371-387.

- Ratcliffe, K.T., Wright, A.M., Spain, D., 2012. Unconventional methods for unconventional plays: using elemental data to understand shale resource plays. *PESA News Resources* – April/May 2012, 55-60.
- Richards, R.E., Mullins, G.L., 2003. Upper Silurian microplankton of the Leinwardine Group, Ludlow Series, in the type Ludlow area and adjacent regions. *Palaeontology* 46, 557-611.
- Saltzman, M.R., 2003. Late Paleozoic ice age: Oceanic gateway or pCO<sub>2</sub>? *Geology* 31, 151–154.
- Saltzman, M.R., 2005. Phosphorus, nitrogen, and the redox evolution of the Paleozoic oceans. *Geology* 33, 573-576.
- Saltzman, M.R., Thomas, E., 2012. Carbon isotope stratigraphy. In: Gradstein, F.M., Ogg, J.G., Schmitz, M.D., Ogg, G.M. (Eds.), *The Geologic Time Scale 2012, Volume 1*. Elsevier. pp. 207-232.
- Samtleben, C., Munnecke, A., Bickert, T., 2000. Development of facies and C/O-isotopes in transects through the Ludlow of Gotland: evidence for global and local influences on a shallow-marine environment. *Facies* 43, 1-38.
- Schmitz, B., Bergström, S.M., 2007. Chemostratigraphy in the Swedish Upper Ordovician: regional significance of the Hirnantian  $\delta^{13}\text{C}$  excursion (HICE) in the Boda Limestone of the Siljan region. *GFF* 129, 133-140.
- Smolarek, J., Trela, W., Bond, D.P.G., Marynowski, L., 2017. Lower Wenlock black shales in the northern Holy Cross Mountains, Poland: sedimentary and geochemical controls on the Ireviken Event in a deep marine setting. *Geological Magazine* 154, 247-264.
- Štorch, P., 1995. Biotic crises and post-crisis recoveries recorded by graptolite faunas of the Barrandian area, Czech Republic. *Geolines* 3, 59-70.

- Štorch, P., Frýda, J., 2012. The late Aeronian graptolite *sedgwickii* Event, associated positive carbon isotope excursion and facies changes in the Prague Synform (Barrandian area, Bohemia). *Geological Magazine* 149, 1089-1106.
- Štorch, P., Manda, Š., Loydell, D.K., 2014. The early Ludfordian *leintwardinensis* graptolite event and the Gorstian–Ludfordian boundary in Bohemia (Silurian, Czech Republic). *Palaeontology* 57, 1003-1043.
- Sullivan, N. B., McLaughlin, P. I., Emsbo, P., Barrick, J. E., Premo, W., 2016. Identification of the late Homerian Mulde Excursion at the base of the Salina Group (Michigan Basin, USA). *Lethaia* 49, 591-603.
- Szymański B., Modliński, Z, 2003 (In Polish). Nowelizacja stratygrafii syluru w wybranych profilach wiertniczych obniżenia bałtyckiego. *Biuletyn Państwowego Instytutu Geologicznego* 405, 109-138.
- Talent, J.A., Mawson, R., Andrew, A.S., Hamilton, P.J., Whitford, D.J., 1993. Middle Palaeozoic extinction events: faunal and isotopic data. *Palaeogeography, Palaeoclimatology, Palaeoecology* 104, 139-152.
- Teller, L., 1997. The subsurface Silurian in the East European platform. *Palaeontologia Polonica* 56, 7-21.
- Tomczykova, E., Tomczyk, H., 1979. Stratigraphy of the Polish Silurian and Lower Devonian and development of the Proto-Tethys. *Acta Palaeontologica Polonica* 24, 165-183.
- Torsvik, T.H., Cocks, L.R.M. New global palaeogeographical reconstructions for the

- Early Palaeozoic and their generation. In: Harper, D.A.T., Servais, T. (Eds.), Early Palaeozoic Biogeography and Palaeogeography. Geological Society, London, Memoirs 38, 5-24.
- Trela, W., 2005. Condensation and phosphatization of the Middle and Upper Ordovician limestones on the Malopolska Block (Poland): Response to paleoceanographic conditions. *Sedimentary Geology* 178, 219-236.
- Trela, W., 2008. Sedimentary and microbial record of the Middle/Late Ordovician phosphogenetic episode in the northern Holy Cross Mountains, Poland. *Sedimentary Geology* 203, 131-142
- Tribovillard, N., Algeo, T.J., Lyons, T., Riboulleau, A., 2006. Trace metals as paleoredox and paleoproductivity proxies: an update. *Chemical Geology* 232, 12-32.
- Underwood, C.J., Crowley, S.F., Marshall, J.D., Brenchley, P.J., 1997. High-resolution carbon isotope stratigraphy of the basal Silurian Stratotype (Dob's Linn, Scotland) and its global correlation. *Journal of the Geological Society, London* 154, 709-718.
- Vandenbroucke, T.R., Ancilletta, A., Fortey, R.A., Verniers, J., 2009. A modern assessment of Ordovician chitinozoans from the Shelve and Caradoc areas, Shropshire, and their significance for correlation. *Geological Magazine*, 146(02), 216-236.
- Vandenbroucke, T.R.A., Recourt, P., Nölvak, J., Nielsen, A.T., 2013. Chitinozoan biostratigraphy of the Upper Ordovician *D. clingani* and *P. linearis* graptolite biozones on the Island of Bornholm, Denmark. *Stratigraphy* 10, 281-301.

- Vandenbroucke, T.R., Emsbo, P., Munnecke, A., Nuns, N., Duponchel, L., Lepot, K., Quijada, M., Paris, F., Servais, T., Kiessling, W., 2015. Metal-induced malformations in early Palaeozoic plankton are harbingers of mass extinction. *Nature Communications* 6, 1-6.
- Walliser, O.H., 1964. Conodonten des Silurs. *Abhandlungen des Hessischen Landesamtes für Bodenforschung* 41, 1-106.
- Wang, K., Chatterton, B.D.E., Wang, Y., 1997. An organic carbon isotope record of Late Ordovician to early Silurian marine sedimentary rocks, Yangtze Sea, South China: Implications for CO<sub>2</sub> changes during the Hirnantian glaciation. *Palaeogeography, Palaeoclimatology, Palaeoecology* 132, 147-158.
- Yan, D., Chen, D., Wang, Q., Wang, J., Wang, Z., 2009. Carbon and sulfur isotopic anomalies across the Ordovician–Silurian boundary on the Yangtze Platform, South China. *Palaeogeography, Palaeoclimatology, Palaeoecology* 274, 32-39.

**Fig. 1.** Composite Silurian carbon isotope ( $\delta^{13}\text{C}_{\text{carb}}$ ) curve integrated with the global chronostratigraphical standard and graptolite, chitinozoan, acritarch and conodont biozonations. The curve here has been modified from Cramer et al. (2011), Melchin et al. (2012), Saltzman and Thomas (2012), McLaughlin et al. (2012), and Cramer et al. (2015). Conodont biozones are modified from Walliser (1964), Jeppsson (1997b), Männik (2007), and Melchin et al. (2012). Graptolite biozones are primarily from Melchin et al. (2012) as is the chitinozoan biozonation. The acritarch zonation is compiled from zones established in the type areas of the Llandovery, Wenlock and Ludlow Series in Wales and the Welsh Borderland, U.K.: Llandovery Series, Hill and Dorning (1984), modified by Davies et al. (2013, 2016); Wenlock Series, Dorning (1981), modified by Molyneux et al. (1996); Ludlow Series, Mullins (2001), Richards and Mullins (2003). The chronostratigraphy is from Melchin et al. (2012).

**Fig. 2.** Map of east-central Europe showing the Silurian palaeogeographical setting and facies distribution (modified from Teller, 1997; Jarochowska and Munnecke, 2015). The position of Grabowiec-6 (N 50° 57' 5.191", E 23° 25' 56.795") and Zwierzyniec-1 (N 50° 44' 14.013", E 23° 07' 24.570") are labelled by shaded circles along with other borehole localities (white circles) that have been studied in earlier published work.

**Fig. 3.** Stratigraphic column, gamma log, and organic carbon isotopes from Grabowiec-6 along with biostratigraphically significant graptolites, acritarchs, and chitinozoans. Chronostratigraphical boundaries are shown to the left of the  $\delta^{13}\text{C}_{\text{org}}$  curve. The abundances of

radiogenic elements Th, U, and K<sub>2</sub>O are plotted to demonstrate depth control for the sampled section.

**Fig. 4.** Gamma log and organic carbon isotopes from Zwierzyniec-1 along with biostratigraphically significant graptolites, chitinozoans, and acritarchs. Chronostratigraphical boundaries are shown to the left of the  $\delta^{13}\text{C}_{\text{org}}$  curve. The abundances of radiogenic elements Th, U, and K<sub>2</sub>O are plotted to demonstrate depth control for the sampled section.

**Fig. 5.** A one-way hierarchical cluster analysis of elemental geochemistry data produced from Grabowiec-6. Inferred genetic and mineralogical controls on major element associations are labelled on the histogram. The plot was generated using R-statistical software, version 3.1.1.

**Fig. 6.** A one-way hierarchical cluster analysis of elemental geochemistry data produced from Zwierzyniec-1. Inferred genetic and mineralogical controls on major element associations are labelled on the histogram. The plot was generated using R-statistical software, version 3.1.1.

**Fig. 7.** A correlation between Grabowiec-6 and Zwierzyniec-1 based on organic carbon isotope data, inorganic geochemistry, and biostratigraphical data. Globally recognized excursions are labelled. Horizontal and vertical scales are consistent between the two wells. The key to curve fill-lines is shown below the Grabowiec-6 panel; they are the same in the Zwierzyniec-1 panel.

**Fig. 8.** An approximate chronostratigraphical correlation between the organic carbon isotope dataset presented here (Grabowiec-6 and Zwierzyniec-1) and published inorganic carbonate carbon isotope data (Kaljo et al., 1997, 1998, 2007; Munnecke and Männik, 2009; Cramer et al., 2010).

ACCEPTED MANUSCRIPT

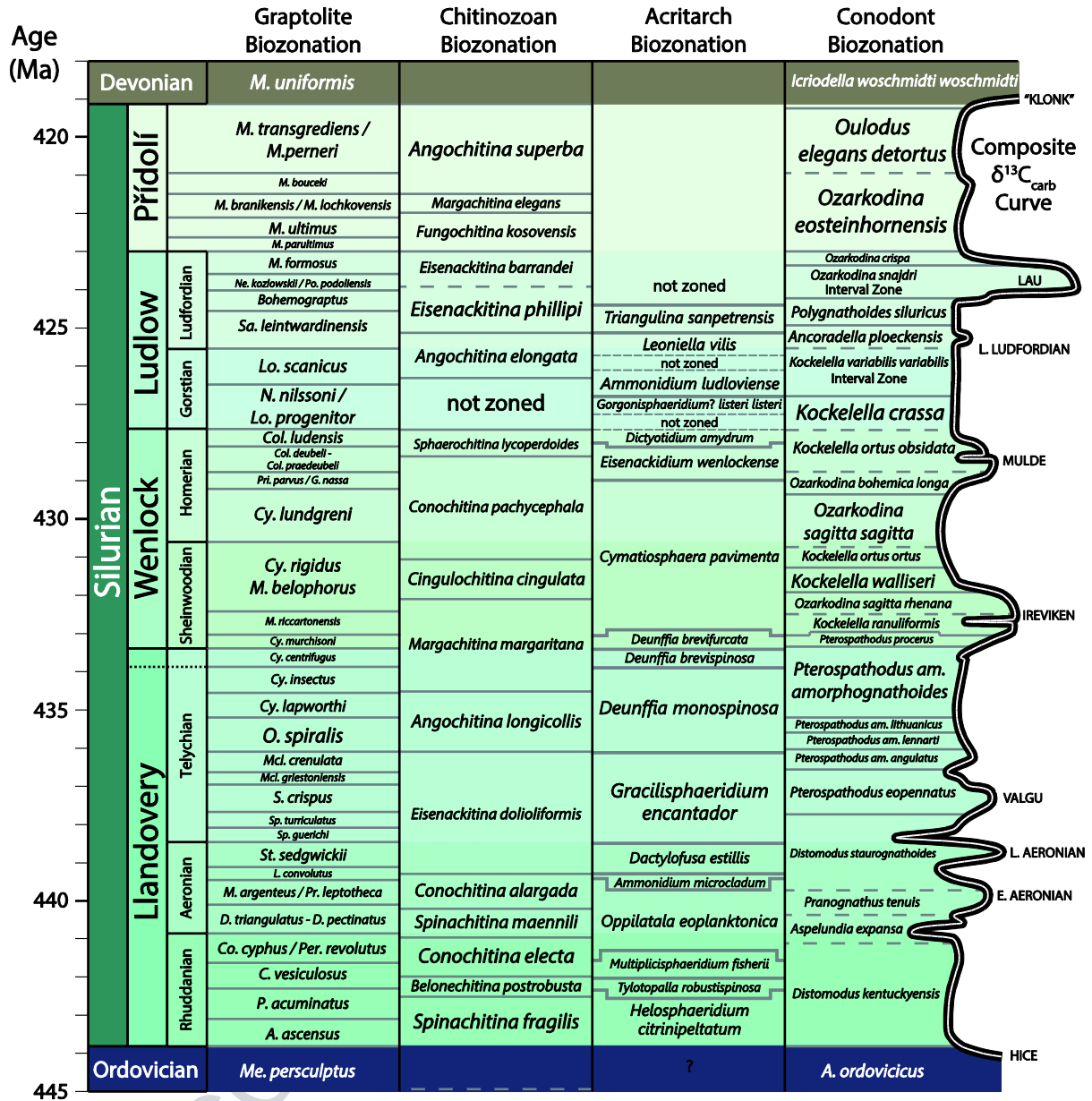
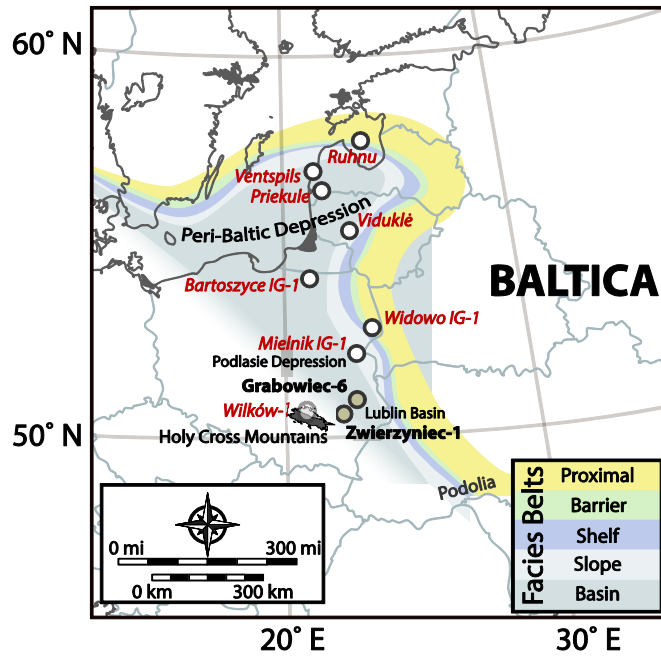


Figure 1



- *Published borehole data*
- **New borehole data**

Figure 2



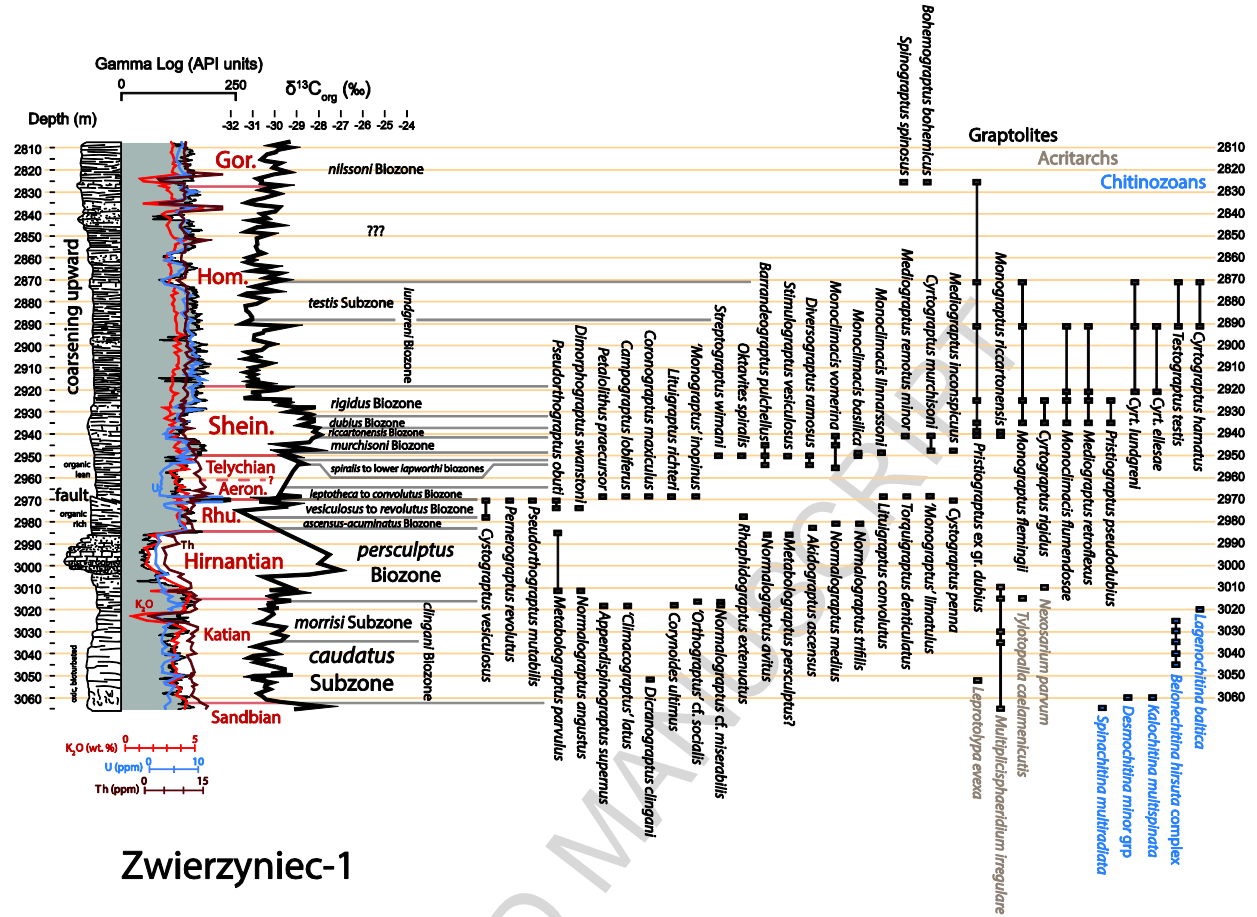


Figure 4

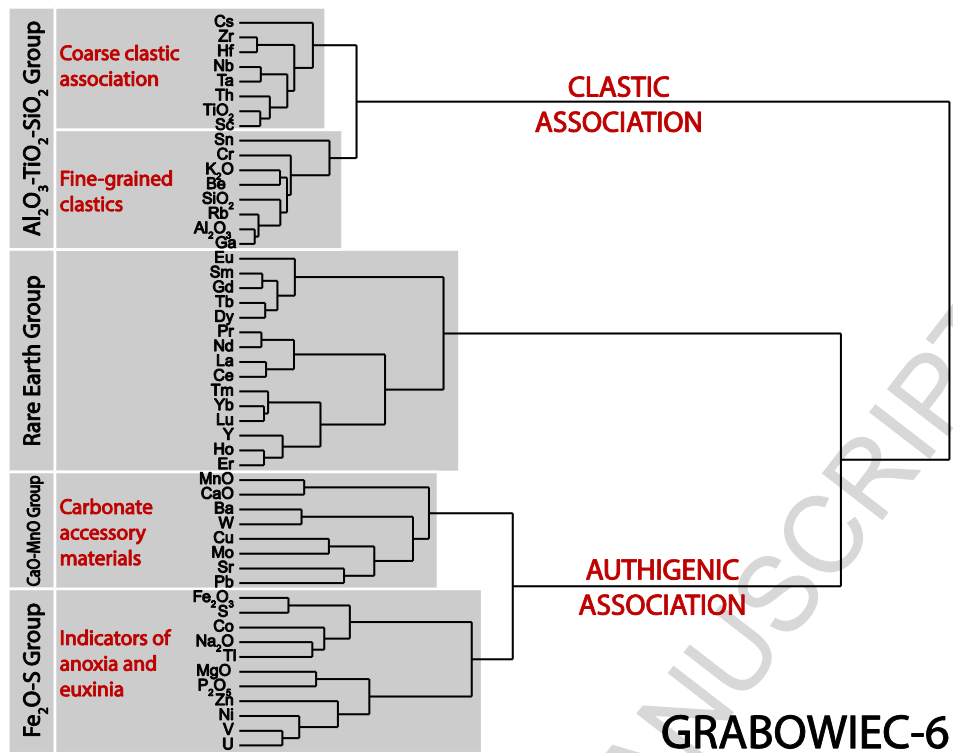


Figure 5

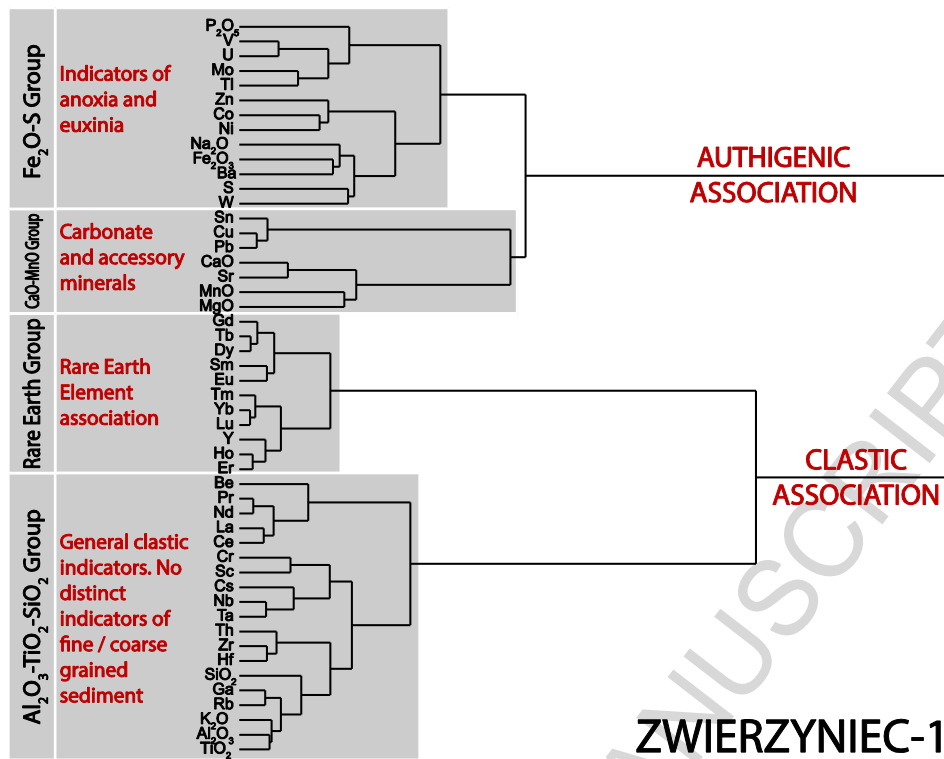


Figure 6

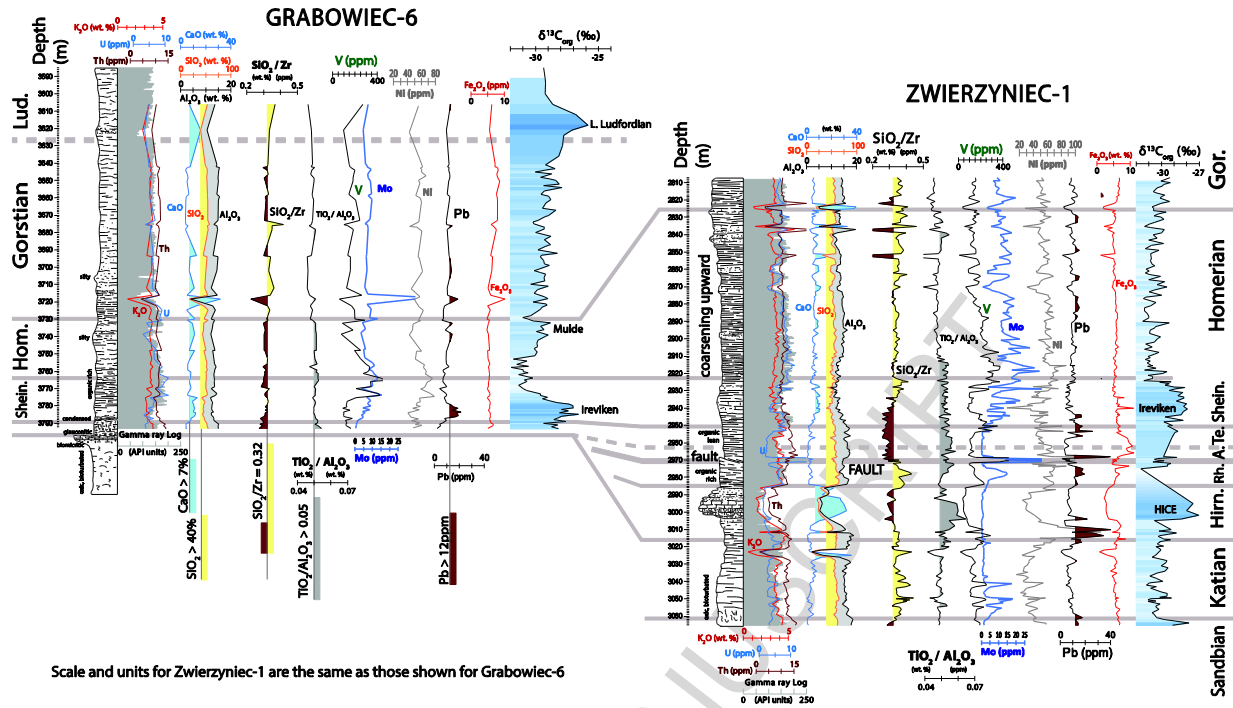


Figure 7

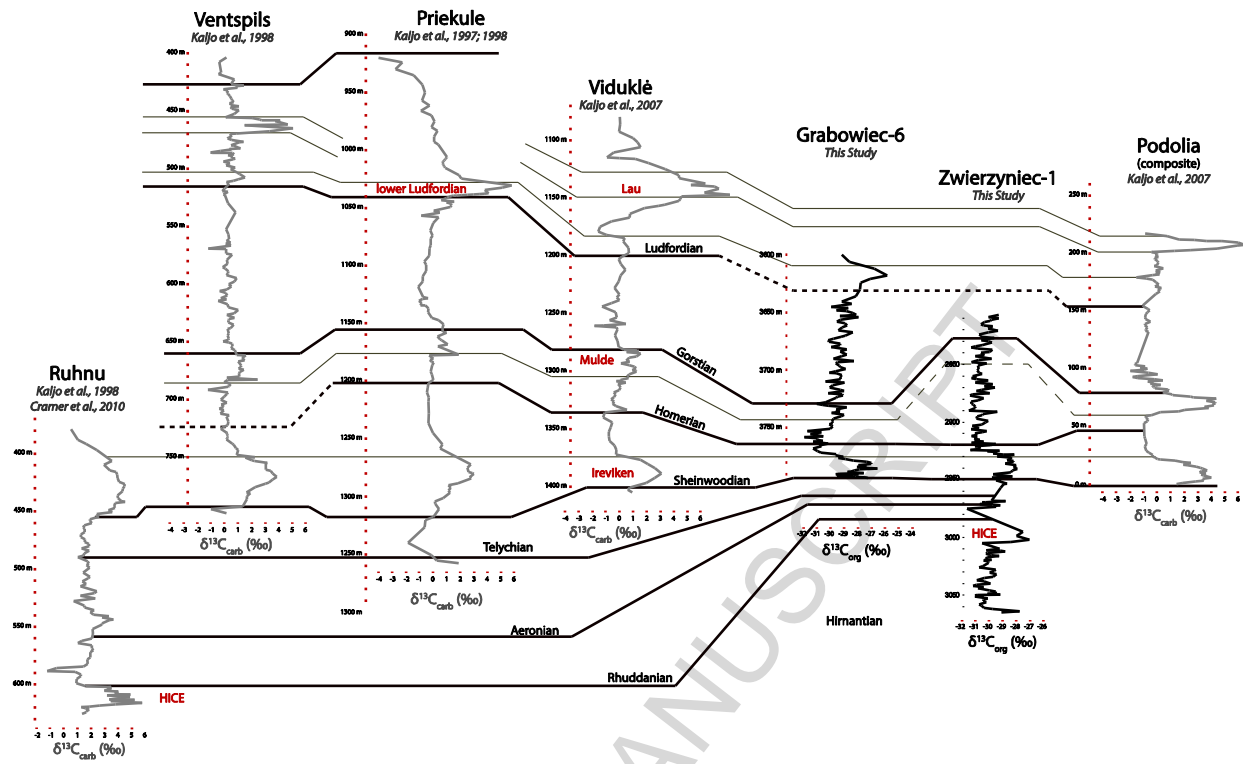


Figure 8

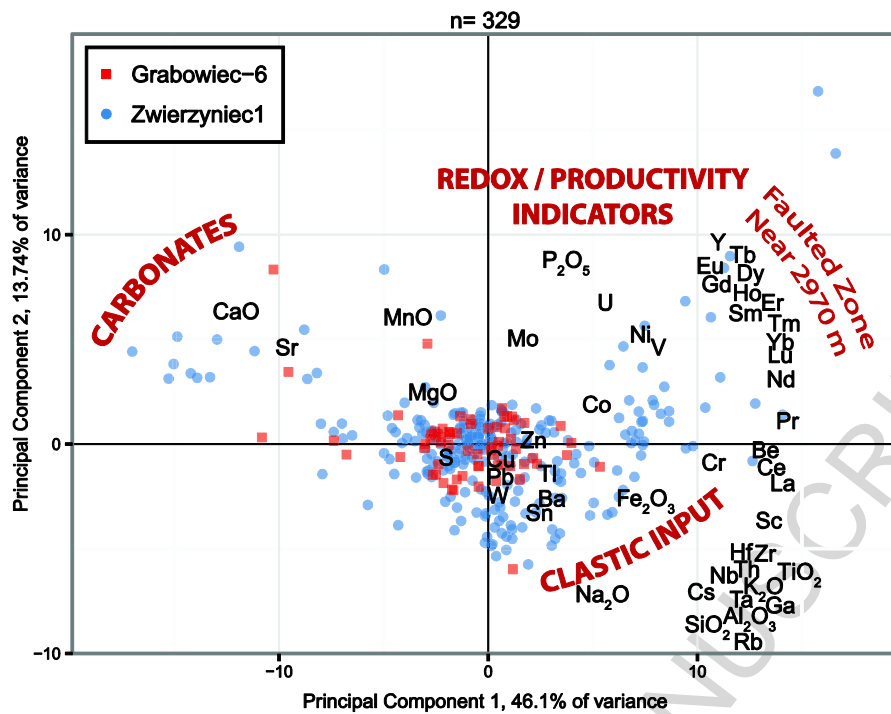


Figure 9

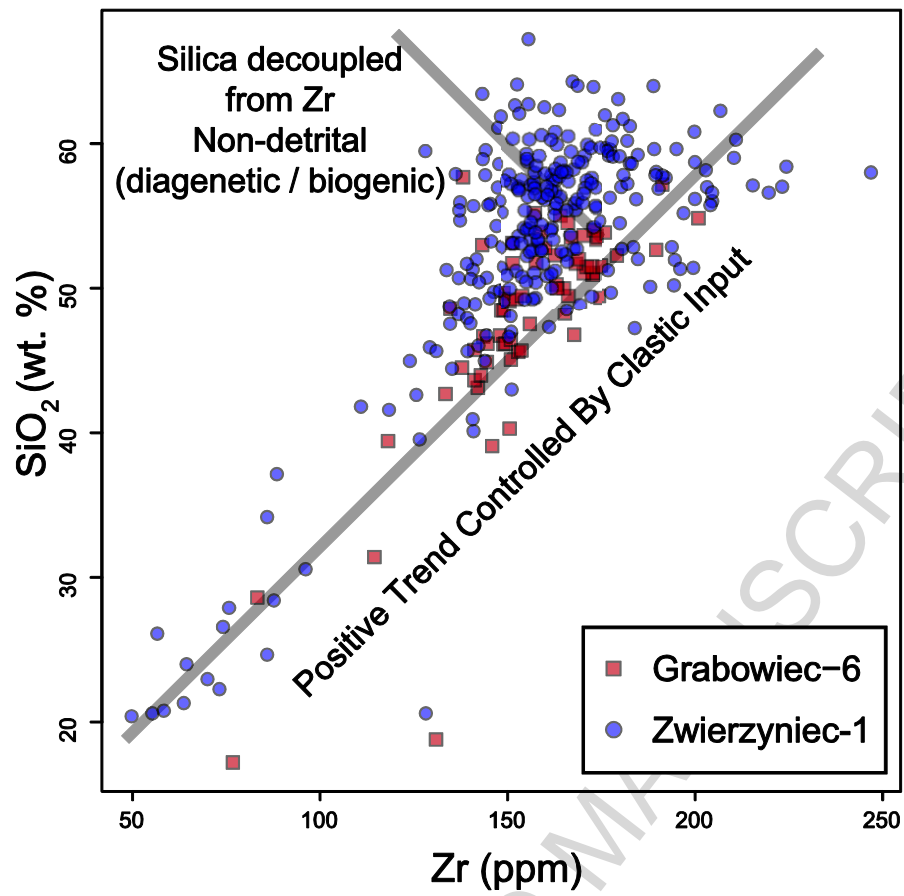


Figure 10

## Highlights

- Two boreholes in central Poland yield a detailed record of ecological change
- Correlations are made from proximal sections into the distal facies of Baltica
- $\delta^{13}\text{C}_{\text{org}}$  data track the features seen in Ordovician-Silurian  $\delta^{13}\text{C}_{\text{carb}}$  curves
- Redox sensitive elements indicate persistent anoxia after the Ireviken Event
- Enrichments heavy metals may be linked with occurrence of malformed palynomorphs

ACCEPTED MANUSCRIPT